

# Photon-pair Generation in Chalcogenide Glass

## Role of Waveguide Linear Absorption

Nuno A. Silva<sup>1,2</sup> and Armando N. Pinto<sup>1,2</sup>

<sup>1</sup>Department of Electronics, Telecommunications and Informatics, University of Aveiro, 3810-193 Aveiro, Portugal

<sup>2</sup>Instituto de Telecomunicações, 3810-193 Aveiro, Portugal

**Keywords:** Quantum Correlated Photon-pairs, Raman Scattering, Spontaneous Four-wave Mixing, Waveguide Absorption.

**Abstract:** We investigate the impact of waveguide loss on the generation rate of quantum correlated photon-pairs through four-wave mixing in a chalcogenide glass fiber. The obtained results are valid even when the photon-pairs are generated in a medium with non-negligible loss,  $\alpha L \gg 1$ . The impact of the loss is quantified through the analysis of the true, total and accidental counting rates at waveguide output. We use the coincidence-to-accidental ratio (CAR) as a figure of merit of the photon-pair source. Results indicate that, the CAR parameter tends to decrease with the increase of the waveguide length, until  $L < 1/\alpha$ . However, a continuous increase of the waveguide length tends to lead to an increase on the CAR value. In that non-negligible loss regime,  $\alpha L \gg 1$ , we are able to observe a significant decrease on the value of all coincidence counting rates. Nevertheless, that decrease is even more pronounced on the accidental counting rate. Moreover, for waveguide length  $L = 10/\alpha$  we are able to obtain a CAR of the order of 70, which is higher than the CAR value for the specific case of  $\alpha = 0$  with  $L = 2$  cm, i.e. CAR=42. This indicates that the waveguide loss can improve the degree of quantum correlation between the photon-pairs.

## 1 INTRODUCTION

Quantum correlated photon-pairs are important resources in the field of quantum communications (Gisin et al., 2002). That correlated photon-pairs can be used to implement heralded single photon sources (Castelletto and Scholten, 2008) or entangled photon sources (Yuan et al., 2010). In both cases, that kind of sources are important elements in quantum key distribution applications (Gisin et al., 2002). The four-wave mixing process (FWM) can provide a solution to obtain quantum correlated photon-pairs already inside of optical waveguides (Fiorentino et al., 2002; Lin et al., 2007). Moreover, when implemented in a chalcogenide glass fiber ( $\text{As}_2\text{S}_3$ ) the FWM process appears as a natural solution to implement on-chip quantum technologies for generation of quantum states (Ta'eed et al., 2007; Eggleton et al., 2012; He et al., 2012). This due to the fact that the chalcogenide glass presents a high value of nonlinear parameter (Lamont et al., 2008), that allows efficient generation of photon-pairs through FWM over very short distances, and an almost negligible two-photon absorption process (Lamont et al., 2008). Moreover, that glass also presents a low Raman-gain window, which

is essential to reduce the generation rate of uncorrelated photons (Xiong et al., 2010; Xiong et al., 2011; Lin et al., 2007), and a high photosensitivity (Eggleton et al., 2012).

Recently, in (Xiong et al., 2010; Xiong et al., 2011; Clark et al., 2012) authors investigate the generation of correlated photon-pairs in  $\text{As}_2\text{S}_3$  chalcogenide glass through FWM process. Nevertheless, those studies were performed in the limit  $L \ll 1/\alpha$ , where  $L$  is the waveguide length, and  $\alpha$  is the loss coefficient. In that regime the loss can be neglected. In this work, we report theoretically the impact of waveguide loss on the generation of quantum correlated photon-pairs through FWM process, in  $\text{As}_2\text{S}_3$  chalcogenide glass fiber. We achieve a coincidence-to-accidental ratio of the 70, for  $\alpha L = 10$  and for a pump power of 0.5 W, at waveguide input. We demonstrate that the difference between total coincidences and true coincidences decreases with the increase of  $\alpha L$ , which can be very important for future implementation of on-chip quantum technologies.

This paper contains four sections. Section 2 deals with the theoretical model that describes the generation of the photon-pairs inside a chalcogenide glass fiber with non-negligible loss through spontaneous

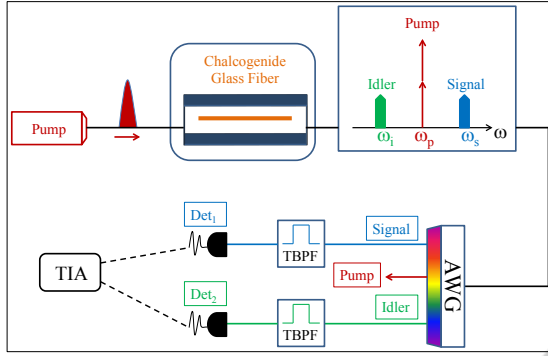


Figure 1: Schematic representation of the spontaneous FWM process in a chalcogenide glass fiber as a source of correlated photon-pairs. Details of the setup are presented in the text.

FWM process. Section 3 reports the obtained theoretical results. The final section summarizes the main conclusions of this work.

## 2 THEORY

In the FWM process, two pump photons ( $\omega_p$ ) are annihilated and two new are created, one at Stokes frequency  $\omega_i$  (know as idler field), and other at anti-Stokes frequency  $\omega_s$  (known as signal field), such that  $2\omega_p = \omega_s + \omega_i$ . In Fig. 1, we present a schematic representation of the spontaneous FWM process in a chalcogenide glass fiber as a source of quantum correlated photon-pairs. Inside the waveguide and simultaneously with the FWM are also generated noise photons through the Raman scattering process. In Fig. 1, an unique pump field is sent a chalcogenide glass fiber in order to induce the spontaneous FWM process. At waveguide output the signal and idler photons generated through FWM and Raman scattering, plus the pump field passes through an arrayed waveguide grating (AWG) to separate the optical fields. The signal photons are spectrally filtered by a tunable band-pass filter (TBPF) centered at  $\bar{\omega}_s$  and collected by the photon counting module, Det<sub>1</sub>. The idler photons passes through a TBPF centered at  $\bar{\omega}_i$  and collected by the photon counting module, Det<sub>2</sub>. The central frequencies of the filters are chosen such that  $2\omega_p = \bar{\omega}_s + \bar{\omega}_i$ . The output signals from the two photon detectors in Fig. 1 are collected by a time interval analyzer (TIA) in order to measure the coincidences.

For a filter bandwidth,  $\Delta\omega_u$ , much narrower than its mid-frequency,  $\Delta\omega_u \ll \omega_u$ , the flux of signal and idler photons at chalcogenide waveguide output is given by (Silva and Pinto, 2012; Silva and Pinto, 2013; Lin et al., 2007)

$$I_u = \langle \hat{A}_u^\dagger(L, \tau) \hat{A}_u(L, \tau) \rangle \approx \Delta v_u \mathcal{F}_u(L), \quad (1)$$

where  $\hat{A}_u(L, \tau)$  is the field annihilation operator, and  $\Delta v_u$  is given by

$$\Delta v_u = \frac{1}{2\pi} \int d\omega_u |H_u(\omega_u - \bar{\omega}_u)|^2 \quad (2)$$

with  $H_u(\omega_u - \bar{\omega}_u)$  being a filter function centered at  $\bar{\omega}_u$ , with  $u = s$  or  $i$  representing the signal or idler field. In (1),  $\mathcal{F}_u(L)$  is given by (Silva and Pinto, 2012; Silva and Pinto, 2013; Lin et al., 2007)

$$\mathcal{F}_u(L) = |v_u(L, 0)|^2 + \alpha_u \mathcal{N}_u \int_0^L dz |\mu_u(L, z)|^2$$

$$+ \alpha_v (\mathcal{N}_v + 1) \int_0^L dz |v_u(L, z)|^2 + (\mathcal{N}_{up} + \Theta_{up}) |g_R(\Omega_{up})| \times \int_0^L dz |\bar{A}_p(z) \mu_u(L, z) - \bar{A}_p^*(z) v_u(L, z)|^2, \quad (3)$$

where  $L$  is the waveguide length,  $\alpha_u$  is the loss coefficient at frequency  $\bar{\omega}_u$  with  $u \neq v = s$  or  $i$  represents the signal or idler field,  $\Theta(-\Omega_{up})$  is the Heaviside step function,

$$\mathcal{N}_u = \frac{1}{\exp\{\hbar\bar{\omega}_u/(k_B T) - 1\}}, \quad (4)$$

and

$$\mathcal{N}_{up} = \frac{1}{\exp\{\hbar|\Omega_{up}|/(k_B T) - 1\}}, \quad (5)$$

where  $\Omega_{up} = \bar{\omega}_u - \omega_p$ ,  $k_B$  is the Boltzmann constant,  $T$  is the waveguide temperature, and  $\hbar = h/(2\pi)$  with  $h$  representing the Planck constant. In (3),  $g_R(\Omega_{up})$  is the Raman gain coefficient,  $A_p$  is the pump field envelope function, such that  $P_p(L) = |A_p(L)|^2$  represents the pump power at a distance  $L$  in the waveguide, and  $v_u(L, z)$  and  $\mu_u(L, z)$  are defined in (Voss et al., 2006; Silva and Pinto, 2012; Silva and Pinto, 2013).

The cross correlation between the signal and idler photons is given by (Silva and Pinto, 2012; Silva and Pinto, 2013; Lin et al., 2007)

$$G_{(st)}^{(2)}(\tau) = \langle \hat{A}_i^\dagger(L, t) \hat{A}_s^\dagger(L, t + \tau) \hat{A}_s(L, t + \tau) \hat{A}_i(L, t) \rangle \approx |\phi_c(\tau)|^2 |\mathcal{F}^c(L, \bar{\omega}_s, \bar{\omega}_i)|^2 + I_i I_s, \quad (6)$$

where  $\phi_c(\tau)$  is the filters cross correlation function

$$\phi_c(\tau) = \frac{1}{2\pi} \int d\omega H_s(\omega - \bar{\omega}_s) H_i(\bar{\omega}_s - \omega) e^{-i\omega\tau}, \quad (7)$$

and (Silva and Pinto, 2012; Silva and Pinto, 2013; Lin et al., 2007)

$$\mathcal{F}^c(L, \bar{\omega}_s, \bar{\omega}_i) = \mu_s(L, 0) v_i(L, 0) + \alpha_s (\mathcal{N}_s + 1) \int_0^L dz \mu_s(L, z) v_i(L, z) + \alpha_i \mathcal{N}_i \int_0^L dz v_s(L, z) \mu_i(L, z) - (\mathcal{N}_{ip} + \Theta_{ip}) |g_R(\Omega_{ip})| \times \int_0^L (\bar{A}_p(z) \mu_s(L, z) - \bar{A}_p^*(z) v_s(L, z)) \times (\bar{A}_p(z) \mu_i(L, z) - \bar{A}_p^*(z) v_i(L, z)) dz. \quad (8)$$

From (6) we can define the total coincidence counting rate,  $R_{cc}$ , the accidental coincidences,  $R_{ac}$ , and the true coincidence counting rate,  $R_{tc}$ , as follows

$$R_{cc} = \int_{t_0}^{t_0+t_c} G_{(si)}^{(2)}(\tau) d\tau \approx \int_{t_0}^{t_0+t_c} |\phi_c(\tau)|^2 d\tau \left( |\mathcal{F}^c(L, \bar{\omega}_s, \bar{\omega}_i)|^2 + I_i I_s \right) \quad (9a)$$

$$R_{ac} = \int_{t_0}^{t_0+t_c} I_i I_s d\tau \approx (\Delta\nu_s \Delta\nu_i) t_c \mathcal{F}_s(L) \mathcal{F}_i(L) \quad (9b)$$

$$R_{tc} = \int_{t_0}^{t_0+t_c} \left( G_{(si)}^{(2)}(\tau) - I_i I_s \right) d\tau \approx \int_{t_0}^{t_0+t_c} |\phi_c(\tau)|^2 d\tau \left( |\mathcal{F}^c(L, \bar{\omega}_s, \bar{\omega}_i)|^2 \right), \quad (9c)$$

where  $t_c$  is the coincidence time window (Lin et al., 2007). Moreover, we can define the coincidence-to-accidental ratio as (Silva and Pinto, 2012; Silva and Pinto, 2013; Lin et al., 2007)

$$\text{CAR} = \frac{R_{cc}}{R_{ac}}, \quad (10)$$

which is a figure of merit of the source of correlated photon-pairs (Chen et al., 2006). We admit that the signal and idler filters are rectangular shaped, and they have the same optical bandwidth,  $\Delta\omega_u = \Delta\omega$ . In that case

$$\phi_c(\tau) = \Delta\omega \text{sinc}\left(\frac{\Delta\omega\tau}{2}\right) e^{-i\bar{\omega}_u\tau}, \quad (11)$$

and

$$\int_0^{t_c} |\phi_c(\tau)|^2 d\tau = 2 \frac{\cos(\Delta\omega t_c) - 1 + (\Delta\omega t_c) \text{Si}(\Delta\omega t_c)}{t_c}, \quad (12)$$

where

$$\text{Si}(\Delta\omega t_c) = \int_0^{\Delta\omega t_c} \text{sinc}(t) dt, \quad (13)$$

is the sine integral function. Moreover,  $\Delta\nu_u$  in (1) is given by  $\Delta\omega_u/(2\pi)$ .

### 3 RESULTS

In this section we present the results for the generation of photon-pairs inside the chalcogenide waveguide through FWM process. We present results for the signal and idler photon fluxes as a function of the frequency detuning between pump and signal fields. We analyze the impact of the waveguide loss on the evolution of the CAR with the frequency detuning between pump and signal field, and with the waveguide

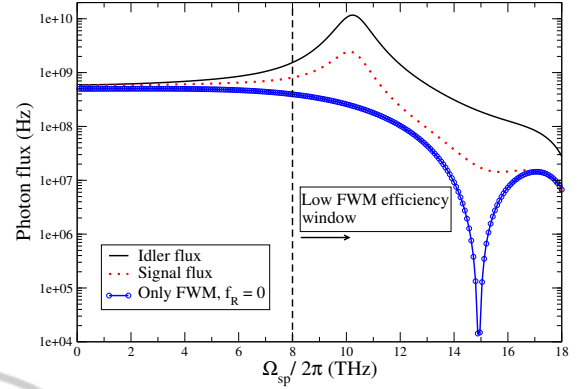


Figure 2: Signal and Idler photon fluxes for  $L = 2$  cm and  $\alpha = 0$ . When  $f_R = 0$ , the Raman scattering process is ignored.

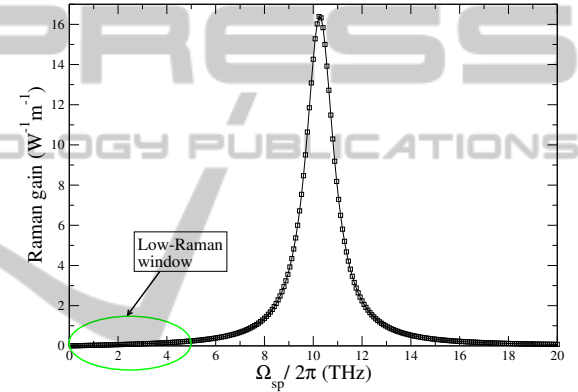


Figure 3: Raman gain coefficient for the chalcogenide glass.

length. Moreover, we also present results for the evolution of the coincidence counts with the waveguide length.

The pump wavelength used in this work is  $\lambda_p = 1550$  nm. We assume that all fields have the same loss coefficient  $\alpha_p = \alpha_s = \alpha_i = 60$  dB/m, and the waveguide nonlinear parameter is  $\gamma = 10$  W<sup>-1</sup>/m (Lamont et al., 2008). The chalcogenide glass fiber group-velocity dispersion at 1550 nm is  $D_c = 29$  ps/nm/km ( $\beta_2 = -3.7 \times 10^{-26}$  s<sup>2</sup>/m) (Lamont et al., 2008). The Raman response functions were taken from (Xiong et al., 2009; Lamont et al., 2008), with  $\tau_1 = 15.5$  fs,  $\tau_2 = 230.5$  fs, and  $f_R = 0.11$ . The chalcogenide glass fiber is at room temperature,  $T = 300$  K. We consider ideal rectangular signal and idler filters with equal bandwidths of  $\Delta\omega/(2\pi) = 50$  GHz, and a coincidence time window of  $t_c = 16$  ps. Finally, we adopt a pump power at chalcogenide waveguide input of  $P_p(0) = 0.5$  W.

In Fig. 2 we present the individual signal and idler photon fluxes given by (1), as a function of pump-signal frequency detuning. In the figure when  $f_R = 0$ ,

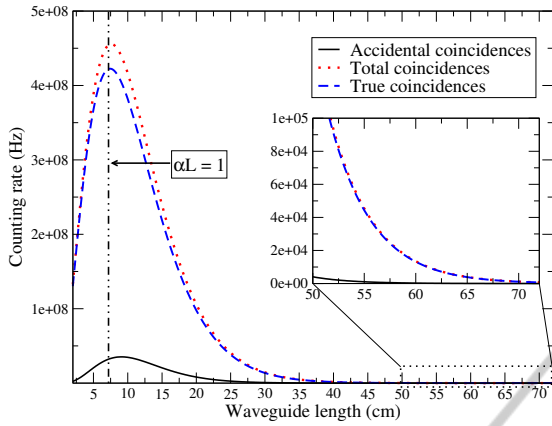


Figure 4: Coincidence counting rate as a function of waveguide length, for  $\Omega_{sp}/2\pi = 1.5$  THz, with  $f_R = 0.11$ .

the Raman scattering process is ignored. It can be seen in Fig. 2 that for small values of frequency detuning most of the photons generated inside the waveguide are due to the FWM process. In that scenario, the photon fluxes for  $f_R = 0.11$  and for  $f_R = 0$  are almost equal. Results also show that, when  $f_R = 0$  the signal and idler photon fluxes rapidly decreases with the increase of the frequency detuning. This is due to the fact that the phase matching condition  $\Delta\beta \approx \Omega_{sp}^2 \beta_2$  in (1) starts to deviates from its minimum value, and consequently the FWM is no longer efficient for high values of frequency detuning (Agrawal, 2001). However, when we consider the Raman scattering process, the signal and idler photon fluxes increase with the increase of the frequency detuning, until  $\Omega_{sp}/2\pi < 10$  THz. That is due to the fact that we are approaching the Raman gain peak for the chalcogenide waveguide. Due to that we define a low efficiency window for the FWM process for  $\Omega_{sp}/2\pi > 8$  THz.

Figure 3 presents the Raman gain coefficient as a function of frequency detuning for the chalcogenide glass fiber. Since the Raman scattering significantly degrades the quality of the correlated photon-pair source (Lin et al., 2007), we identify two ideal regimes where the Raman gain coefficient assumes a small value,  $\Omega_{sp}/2\pi < 5$  THz, and  $\Omega_{sp}/2\pi > 16$  THz. From Fig. 2 and Fig. 3, we can define a frequency region,  $\Omega_{sp}/2\pi < 5$  THz, where the FWM is highly efficient, and the Raman scattering process exhibits low efficiency window.

Figure 4 presents the evolution of the  $R_{cc}$ ,  $R_{ac}$ , and  $R_{tc}$  parameters given by (9), with the waveguide length,  $L$ . Results show that, all the counting rates presented in Fig. 4 increases with the increase of  $L$ , until  $L \approx 1/\alpha$ . The increase of  $R_{ac}$  with the waveguide length (and consequently the increase of  $R_{cc}$ ) is due to the stimulated FWM and Raman scattering processes, which generate uncorrelated photons.

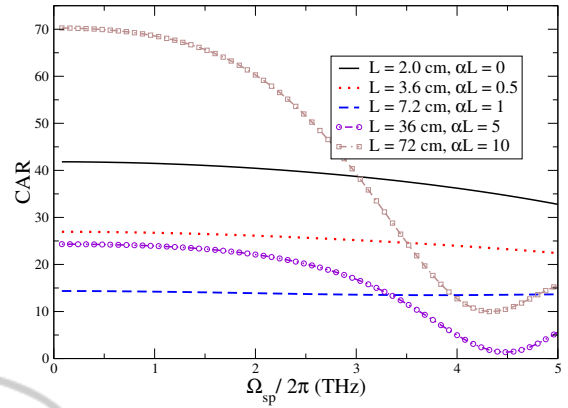


Figure 5: Coincidence-to-Accidental ratio as a function of frequency detuning, with  $f_R = 0.11$ .

The increase of  $R_{tc}$  with  $L$  is due to the increase of the FWM efficiency with the waveguide length. Nevertheless, the increase of the accidental coincidences with the waveguide length is much lower than the increase of the total and true coincidences. It can also be seen in Fig. 4 that, a continuous increase of  $L$  leads to a rapidly decrease of all counting rates. This is due to the waveguide loss coefficient that starts to absorb most of the generated photons inside the waveguide. Moreover, the loss coefficient also decrease the pump power that evolves in the waveguide, which avoids the generation of photons from stimulated FWM process and Raman scattering. For  $\alpha L \gg 1$  the effective waveguide length is much smaller than its length. It can also be seen in the inset present in Fig. 4 that, when  $L \gg 1/\alpha$  the  $R_{cc}$  and the  $R_{tc}$  parameters are almost equal. Moreover, in that regime the accidental counting rate is almost negligible when compared with  $R_{cc}$  or  $R_{tc}$ . This mean that, for  $L \gg 1/\alpha$  most of the photons at waveguide output are signal-idler pairs, which reveals the high purity nature of the photon-pair source in this non-negligible loss regime.

Figure 5 presents the CAR given by (10) as a function of frequency detuning, for several values of waveguide length. In Fig. 5 we also present results for the specific case  $\alpha = 0$  and  $L = 2$  cm. Results show that for all cases the CAR parameter tends to decrease with the increase of  $\Omega_{sp}/2\pi$ . This is due to the loss of efficiency of the FWM process with the evolution of the frequency detuning. Results also show that for small values of  $\Omega_{sp}/2\pi$ , the CAR value decreases with the increase of  $\alpha L$ , until  $\alpha L = 1$ . After, the CAR starts to increase, and for  $\alpha L = 10$ , we are able to obtain CAR=70, which is much more higher than the CAR for  $\alpha = 0$  and  $L = 2$  cm, CAR=42. This is due to the fact, increasing the waveguide length the  $R_{ac}$  parameter tends to zero more rapidly than the  $R_{cc}$  or  $R_{tc}$  parameters. Moreover, the results present in

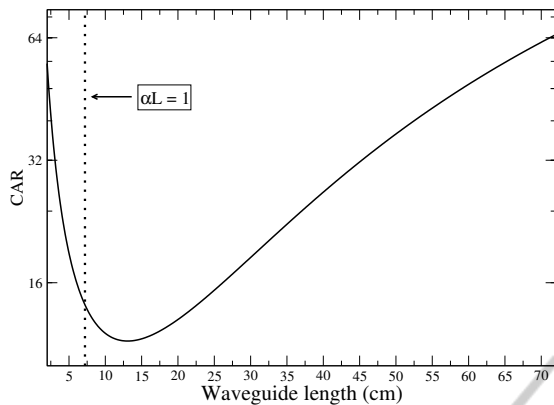


Figure 6: Coincidence-to-Accidental ratio as a function of waveguide length, for  $\Omega_{sp}/2\pi = 1.5$  THz, with  $f_R = 0.11$ .

Fig. 5 are in line with recent reported experimental results for the CAR parameter in waveguides with non-negligible loss coefficient (Xiong et al., 2012).

Finally, in Fig. 6 we present the evolution of the CAR with the waveguide length. Results show that the CAR decreases with the increase of  $L$ , until  $L \approx 1/\alpha$ . That decrease of the CAR with  $L$  is due to the increase on the probability of generating signal and idler photons through stimulated FWM. That evolution of the CAR parameter is in line with previous reported experimental results (Harada et al., 2010). Nevertheless, a continuous increase of  $L$  tends to lead to an increase of the CAR, until  $L \leq 10/\alpha$ . This is due to the fact that  $R_{ac}$  decreases more rapidly with  $L$  than  $R_{cc}$ , see Fig. 4. When  $L \gg 1/\alpha$ , the CAR assumes an equal or even a higher value than when  $L \leq 1/\alpha$ . In that non-negligible loss regime the waveguide absorbs most of the pump photons, decreasing in that case the probability of generating uncorrelated photons from stimulated FWM and Raman scattering processes.

## 4 CONCLUSIONS

In summary, we investigate the impact of linear loss on the generation of quantum correlated photon-pairs in a chalcogenide glass fiber. We define a frequency regime where the FWM is highly efficient and the Raman gain coefficient assumes a small value. We show that the CAR value decrease with the increase of the frequency detuning between pump and signal field, due to the loss of efficiency of the FWM process. Moreover, the CAR parameter tends to decrease with the increase of  $\alpha L$ , until  $L \lesssim 1/\alpha$ . That decrease on the CAR parameter is mainly due to the increase of the accidental counting rate. The increase of the accidental counting rate with the waveguide length is due to the generation of uncorrelated photons through

stimulated FWM and Raman scattering. After that,  $\alpha L > 1$ , the CAR parameter tends to increase with the continuous increase of the waveguide length, until  $\alpha L = 10$ . In a non-negligible loss regime,  $\alpha L > 1$ , the total and true coincidence counting rates tends to be equal, which leads to an increase on the CAR value. In that case, our findings show that the presence of a waveguide with non-negligible loss parameter tends to improve the quality of the source, when compared with the limit  $\alpha = 0$ . More specifically, for  $\alpha L = 10$  we are able to obtain a CAR value higher than for  $\alpha L = 0$ , with  $L = 2$  cm.

In waveguides with non-negligible loss we observe a significantly decrease on the generation rate of signal-idler photon pairs, when compared with the regime  $\alpha L \ll 1$ . Nevertheless, in that regime our analysis shows that the coincidence counting rate can be higher than 10 kHz, for a CAR value of the order of 70.

## ACKNOWLEDGEMENTS

This work was supported in part by the FCT - Fundação para a Ciência e a Tecnologia, through the PhD Grant SFRH/BD/63958/2009, by the FCT and European Union FEDER - Fundo Europeu de Desenvolvimento Regional, through project PTDC/EEA-TEL/103402/2008 (QuantPrivTel), and by the FCT and the Instituto de Telecomunicações, under the PEst-OE/EEI/LA0008/2011 program, project “P-Quantum”.

## REFERENCES

- Agrawal, G. (2001). *Nonlinear Fiber Optics*. Academic Press, 3 edition.
- Castelletto, S. A. and Scholten, R. E. (2008). Heralded single photon sources: a route towards quantum communication technology and photon standards. *The European Physical Journal Applied Physics*, 41:181–194.
- Chen, J., Lee, K. F., Liang, C., and Kumar, P. (2006). Fiber-based telecom-band degenerate-frequency source of entangled photon pairs. *Opt. Lett.*, 31(18):2798–2800.
- Clark, A. S., Collins, M. J., Judge, A. C., Mägi, E. C., Xiong, C., and Eggleton, B. J. (2012). Raman scattering effects on correlated photon-pair generation in chalcogenide. *Opt. Express*, 20:16807–16814.
- Eggleton, B., Vo, T., Pant, R., Schr, J., Pelusi, M., Yong Choi, D., Madden, S., and Luther-Davies, B. (2012). Photonic chip based ultrafast optical processing based on high nonlinearity dispersion engineered chalcogenide waveguides. *Laser & Photonics Reviews*, 6:97–114.

- Fiorentino, M., Voss, P., Sharping, J., and Kumar, P. (2002). All-fiber photon-pair source for quantum communications. *Photonics Technology Letters, IEEE*, 14(7):983–985.
- Gisin, N., Ribordy, G., Tittel, W., and Zbinden, H. (2002). Quantum cryptography. *Rev. Mod. Phys.*, 74(1):145–195.
- Harada, K., Takesue, H., Fukuda, H., Tsuchizawa, T., Watanabe, T., Yamada, K., Tokura, Y., and Itabashi, S. (2010). Frequency and polarization characteristics of correlated photon-pair generation using a silicon wire waveguide. *Selected Topics in Quantum Electronics, IEEE Journal of*, 16(1):325–331.
- He, J., Xiong, C., Clark, A. S., Collins, M. J., Gai, X., Choi, D.-Y., Madden, S. J., Luther-Davies, B., and Eggleton, B. J. (2012). Effect of low-Raman window position on correlated photon-pair generation in a chalcogenide  $\text{Ge}_{11.5}\text{As}_{24}\text{Se}_{64.5}$  nanowire. *Journal of Applied Physics*, 112:123101.
- Lamont, M. R., Luther-Davies, B., Choi, D.-Y., Madden, S., and Eggleton, B. J. (2008). Supercontinuum generation in dispersion engineered highly nonlinear ( $\gamma = 10/\text{w/m}$ )  $\text{As}_2\text{S}_3$  chalcogenide planar waveguide. *Opt. Express*, 16:14938–14944.
- Lin, Q., Yaman, F., and Agrawal, G. P. (2007). Photon-pair generation in optical fibers through four-wave mixing: Role of Raman scattering and pump polarization. *Phys. Rev. A*, 75(2):023803.
- Silva, N. and Pinto, A. (2013). Effects of losses and nonlinearities on the generation of polarization entangled photons. *Lightwave Technology, Journal of*, 31:1309–1317.
- Silva, N. A. and Pinto, A. N. (2012). Role of absorption on the generation of quantum-correlated photon pairs through FWM. *Quantum Electronics, IEEE Journal of*, 48:1380–1388.
- Ta'eed, V., Baker, N. J., Fu, L., Finsterbusch, K., Lamont, M. R. E., Moss, D. J., Nguyen, H. C., Eggleton, B. J., Choi, D.-Y., Madden, S., and Luther-Davies, B. (2007). Ultrafast all-optical chalcogenide glass photonic circuits. *Opt. Express*, 15:9205–9221.
- Voss, P. L., Köprülü, K. G., and Kumar, P. (2006). Raman-noise-induced quantum limits for  $\chi(3)$  nondegenerate phase-sensitive amplification and quadrature squeezing. *J. Opt. Soc. Am. B*, 23(4):598–610.
- Xiong, C., Helt, L. G., Judge, A. C., Marshall, G. D., Steel, M. J., Sipe, J. E., and Eggleton, B. J. (2010). Quantum-correlated photon pair generation in chalcogenide  $\text{As}_2\text{S}_3$  waveguides. *Opt. Express*, 18(15):16206–16216.
- Xiong, C., Magi, E., Luan, F., Dekker, S., Sanghera, J., Shaw, L., Aggarwal, I., and Eggleton, B. (2009). Raman response in chalcogenide  $\text{As}_2\text{S}_3$  fiber. In *Opto-Electronics and Communications Conference, 2009. OECC 2009. 14th*, pages 1–2.
- Xiong, C., Marshall, G. D., Peruzzo, A., Lobino, M., Clark, A. S., Choi, D.-Y., Madden, S. J., Natarajan, C. M., Tanner, M. G., Hadfield, R. H., Dorenbos, S. N., Zijlstra, T., Zwiller, V., Thompson, M. G., Rarity, J. G., Steel, M. J., Luther-Davies, B., Eggleton, B. J., and O'Brien, J. L. (2011). Generation of correlated photon pairs in a chalcogenide  $\text{As}_2\text{S}_3$  waveguide. *Applied Physics Letters*, 98(5):051101.
- Xiong, C., Monat, C., Collins, M., Tranchant, L., Petiteau, D., Clark, A., Grillet, C., Marshall, G., Steel, M., Li, J., O'Faolain, L., Krauss, T., and Eggleton, B. (2012). Characteristics of correlated photon pairs generated in ultracompact silicon slow-light photonic crystal waveguides. *Selected Topics in Quantum Electronics, IEEE Journal of*, 18(6):1676–1683.
- Yuan, Z.-S., Bao, X.-H., Lu, C.-Y., Zhang, J., Peng, C.-Z., and Pan, J.-W. (2010). Entangled photons and quantum communication. *Physics Reports*, 497:1–40.